Engineering NADH/NAD$^+$ ratio in Halomonas bluephagenesis for enhanced production of polyhydroxyalkanoates (PHA)

Ling, Chen; Qiao, Guan Qing; Shuai, Bo Wen; Olavarria, Karel; Yin, Jin; Xiang, Rui Juan; Song, Kun Nan; Shen, Yun Hao; Guo, Yingying; Chen, Guo Qiang

DOI
10.1016/j.ymben.2018.09.007

Publication date
2018

Document Version
Accepted author manuscript

Published in
Metabolic Engineering

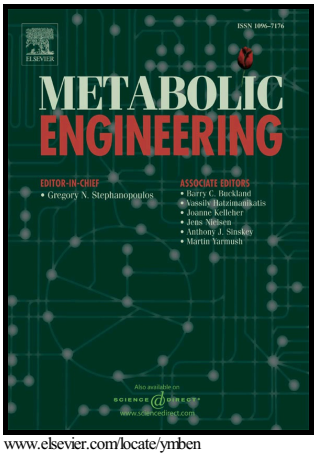

www.elsevier.com/locate/ymben

Engineering NADH/NAD$^+$ Ratio in *Halomonas bluephagenesis* for Enhanced Production of Polyhydroxyalkanoates (PHA)

Chen Ling, Guan-Qing Qiao, Bo-Wen Shuai, Karel Olavarria, Jin Yin, Rui-Juan Xiang, Kun-Nan Song, Yun-Hao Shen, Yingying Guo, Guo-Qiang Chen

PII: S1096-7176(18)30291-X
DOI: https://doi.org/10.1016/j.ymben.2018.09.007
Reference: YMBEN1468

To appear in: *Metabolic Engineering*

Received date: 20 July 2018
Revised date: 12 September 2018
Accepted date: 12 September 2018

Cite this article as: Chen Ling, Guan-Qing Qiao, Bo-Wen Shuai, Karel Olavarria, Jin Yin, Rui-Juan Xiang, Kun-Nan Song, Yun-Hao Shen, Yingying Guo and Guo-Qiang Chen, Engineering NADH/NAD$^+$ Ratio in *Halomonas bluephagenesis* for Enhanced Production of Polyhydroxyalkanoates (PHA), *Metabolic Engineering,* https://doi.org/10.1016/j.ymben.2018.09.007

Original paper

Engineering NADH/NAD$^+$ Ratio in *Halomonas bluephagenesis* for Enhanced Production of Polyhydroxyalkanoates (PHA)

Chen Ling[a], Guan-Qing Qiao[a], Bo-Wen Shuai[a], Karel Olavarria[e], Jin Yin[b], Rui-Juan Xiang[f], Kun-Nan Song[a], Yun-Hao Shen[a], Yingying Guo[a,b*], Guo-Qiang Chen[a,b,c,d*]

[a] Center for Synthetic and Systems Biology, School of Life Sciences, Tsinghua University, Beijing 100084, China

[b] Tsinghua-Peking Center for Life Sciences, School of Life Sciences, Tsinghua University, Beijing 100084, China

[c] MOE Key Lab of Bioinformatics, Center for Nano and Micro Mechanics, Tsinghua University, Beijing 100084, China

[d] MOE Key Lab of Industrial Biocatalysis, Tsinghua University, Beijing 100084, China

[e] Department of Biotechnology, Faculty of Applied Sciences, Delft University of Technology. Department of Biotechnology Building 58, Van der Maasweg 9, Postal code: 2629 HZ, Delft, The Netherlands

[f] Bluepha Co., Ltd., Beijing 102206, China

Corresponding authors:

*Guo-Qiang Chen: chengq@mail.tsinghua.edu.cn (Chen GQ)

School of Life Sciences, Tsinghua University, Beijing 100084, China.

*Yingying Guo: guoyingying@phalab.org (Guo YY)

School of Life Sciences, Tsinghua University, Beijing 100084, China.

Abstract

Halomonas bluephagenesis has been developed as a platform strain for the next generation industrial biotechnology (NGIB) with advantages of resistances to microbial contamination and high cell density growth (HCD), especially for production of polyhydroxyalkanoates (PHA) including poly(3-hydroxybutyrate) (PHB), poly(3-hydroxybutyrate-co-4-hydroxybutyrate) (P34HB) and poly(3-hydroxybutyrate-co-3-hydroxyvalerate) (PHBV). However, little is known about the mechanism behind PHA accumulation under oxygen limitation. This study for the first time found that *H. bluephagenesis* utilizes NADH instead of NADPH as a cofactor for PHB production, thus revealing the rare situation of enhanced PHA accumulation under oxygen limitation. To increase NADH/NAD^+ ratio for enhanced PHA accumulation under oxygen limitation, an electron transport pathway containing electron transfer flavoprotein subunits α and β encoded by *etf* operon was blocked to increase NADH supply, leading to 90% PHB accumulation in the cell dry weight (CDW) of *H. bluephagenesis* compared with 84% by the wild type. Acetic acid, a cost-effective carbon source, was used together with glucose to balance the redox state and reduce inhibition on pyruvate metabolism, resulting in 22% more CDW and 94% PHB accumulation. The cellular redox state changes induced by the addition of acetic acid increased 3HV ratio in its copolymer PHBV from 4% to 8%, 4HB in its copolymer P34HB from 8% to 12%, respectively, by engineered *H. bluephagenesis*. The strategy of systematically modulation on the redox potential of *H. bluephagenesis* led to enhanced PHA accumulation and controllable monomer ratios in PHA copolymers under oxygen limitation, reducing energy consumption and scale-up complexity.

Keywords

NADH, NADH/NAD^+, Oxygen limitation, *Halomonas*, PHB, Polyhydroxyalkanoates, Next Generation Industrial Biotechnology, *etf*

1. Introduction

Polyhydroxyalkanoates (PHA) as biodegradable plastics with structure diversity have been reported to be accumulated by approximately 300 different species of bacteria as well as their recombinants (Lee, 1996; Steinbüchel, 1991; Ferre-Guell and Winterburn 2018; Koller et al., 2017; Le Meur et al., 2014). PHA serve not only as a reserve of carbon and energy source but also as a sink for reducing power (Anderson and Dawes, 1990; Lee, 1996; Senior and Dawes, 1971). PHB is the most abundant and best-studied form of PHA. PHB is synthesized from acetyl-CoA to acetoacetyl-CoA and then 3-hydroxybutyryl-CoA (Steinbüchel and Valentin, 1995), during which acetoacetyl-CoA reductase (AAR, also PhaB) consumes one NADH or NADPH to convert acetoacetyl-CoA to 3-β-hydroxybutyrate-CoA (3HB-CoA).

Most bacteria able to accumulate PHB possess the NADPH dependent PhaB, which consumes one NADPH to convert acetoacetyl-CoA to 3HB-CoA. While *Azotobacter beijerinckii* and *Allochromatium vinosum* were reported to have a NADH consumable PhaB (Matthias and Alexander, 2005; Ritchie et al., 1971; Senior and Dawes, 1973). The NADPH binding sites in PhaB of *Cupriavidus necator* have been identified in the recently solved structure (Kim et al., 2014; Matsumoto et al., 2013). Although chemically very similar, the redox cofactors NADH and NADPH serve distinct biochemical functions: NADPH plays an essential role for the anabolic reduction, while NADH participates in respiration and fermentation under rich oxygen and limited oxygen supply, respectively (Sauer et al., 2004). In *E. coli,* NADPH is mainly generated from the oxidative pentose phosphate (OPP) pathway, the tricarboxylic acid (TCA) cycle due to NADPH-dependent isocitrate dehydrogenase, and the transhydrogenase catalytic reaction, providing 35-45, 20-25, and 30-45 % of total NADPH during the aerobic growth on glucose, respectively (Sauer et al., 2004). Although 35 to 45% NADPH was produced by the OPP pathway via glycolysis, most NADPH was generated from oxygen dependent pathway, especially in bacteria with Entner-Doudoroff (ED) pathway for the central carbon metabolism, in which very limited metabolic flux enters NADPH-producing OPP

pathway (Sauer et al., 2004). The ED, instead of EMP and OPP, has been proven the primary pathway for glucose catabolism in *H. bluephagenesis* (Qin et al., 2018), thus NADPH generation largely depends on the TCA cycle, which requires oxygen. In contrast, NADH can be easily generated via several pathways regardless of the presence of oxygen (San et al., 2002). An excess amount of NADH is formed during glycolysis and degradation of pyruvate to acetyl-CoA in the presence of sufficient glucose, respectively. Very few bacteria contain NADH dependent PhaB to allow majority of the reducing equivalent to sink into PHB and NAD^+, which in turn promotes glycolysis and pyruvate metabolism under oxygen limitation condition (Farhana et al., 2010).

The limitations on essential nutrients (such as N, P, S, Fe and Mg) and presence of sufficient carbon source are critical for most known NADPH dependent species to accumulate PHA (Steinbüchel, 1991). While oxygen limitation has been proven functional for inducing PHA synthesis only in *A. beijerinckii* and recombinant *Saccharomyces cerevisiae* harboring *pha*CAB genes from *A. vinosum,* as both contain NADH consumable PhaB (Portugal-Nunes et al., 2017; de las Heras et al., 2016; Jackson and Dawes, 1976; Senior and Dawes, 1971; Senior and Dawes, 1973).

Oxygen limitation was also mentioned in a fermentation of *C. necator* producing PHB from hydrogen and carbon dioxide instead of glucose (Ishizaki and Tanaka, 1990, 1991; Vollbrecht et al., 1979, 1978; Vollbrecht and Schlegel, 1978), and as high as 62 g/L of P(3HB) was produced in a specially designed fermentor (Ishizaki et al., 1992). While the oxygen limitation mentioned in these studies was based on the relative condition compared with their previous works. For example, in the study of Ishizaki and Tanaka (1990), the aeration was 2 *vvm* (air volume/culture volume/min) under an agitation of 1400 rpm. With an oxygen partial pressure set at 0.15-0.25 atm (the standard atmosphere), the dissolved oxygen (DO) concentration was very high compared with conditions in other related studies. In addition, the oxidation of hydrogen requires a lot of oxygen, and the bioreactors were specially designed, it was

difficult to compare the DO with other studies although oxygen limitation was mentioned.

A random disruption on respiratory NADH consumption was reported to increase NADH/NAD^+ ratio in *A. beijerinckii*, resulting in enhanced PHB accumulation without limitations on essential nutrients in complex substrates such as molasses, while the NADPH consumption rate was essentially the same (Steinbüchel, 1991). This indicates that PHB accumulation can be a fermentation process under oxygen limitation directly consuming NADH generated from glycolysis and pyruvate metabolism (Farhana et al., 2010).

The PHB accumulation depends mostly on acetyl-CoA sourced from TCA cycle or glycolysis (Anderson and Dawes, 1990). The flux of acetyl-CoA toward NADPH dependent anabolic PHB synthesis mainly depends on imbalanced carbon/nitrogen ratio, it is an aerobic process. Whereas oxygen limitation is the key factor for the NADH dependent fermentation process, NADH/NAD^+ ratio increases significantly under oxygen limitation. Citrate synthase has been reported to be inhibited by NADH, as a result acetyl-CoA can no longer enter the TCA cycle, instead, it is channeled to the NADH consuming PHB synthesis pathway (Anderson and Dawes, 1990; de las Heras et al., 2016; Farhana et al., 2010; Jackson and Dawes, 1976; Lee, 1996; Steinbüchel, 1991).

Unlike the NADH consuming PHB fermentation pathway, many other bioproducts, such as 4-hydroxybutyrate and 3-hydroxyvalerate, are derived from 2-oxoglutarate and succinyl-CoA of the TCA cycle. Previously, the R163L mutation on the gene encoding citrate synthase in *E. coli* was reported to reduce inhibition by NADH and therefore improved TCA-cycle flux, leading to enhanced accumulation of 4-hydroxybutyrate and 1,4-butanediol. (Choi et al., 2016; Yim et al., 2011). The systematical modulations and In-silico-driven of the metabolic flux into PHA synthesis pathway were reported in *Pseudomonas putida* (Beckers et al., 2016; Borrero-de Acuña et al., 2014; Christoph Wittmann Anabolism NADPH NADH,

2005; Poblete-Castro et al., 2013). However, we have been unable to find any study to control the monomer ratios in copolymers via systematically modulating the redox state.

Among many PHA producing *Halomonas* spp. (Kucera et al., 2018), *H. bluephagenesis* TD01, as a Gram-negative bacterium, has been reported to engineered for accumulating PHB, copolymers of 3-hydroxybutyrate and 4-hydroxybutyrate (P34HB) and copolymers of 3-hydroxybutyrate and 3-hydroxyvalerate (PHBV) in high density growth cells via fed batch fermentation within 48 h (Chen and Jiang, 2018; Chen et al., 2017; Fu et al., 2014; Tan et al., 2014). Contamination free, high cell density and high PHA content have long been its attractions that are achieved under oxygen limitation (Ye et al 2018b). Compared with other reported PHA producing strains, the aeration or agitation during growth of *H. bluephagenesis* TD01 is much more approachable, the maximal agitations of 800 rpm (revolutions per minute), 280 rpm, 170 rpm, and a constant aeration rate of 1 *vvm* (air volume/culture volume/min), 1 *vvm*, 0.85 *vvm* for 7.5 L, 1 m^3 and 5 m^3 bioreactors, can satisfy the high cell density growth, respectively (Ye et al., 2018b; Kim Beom et al., 2004; Lee, 1996; Steinbüchel, 1991). The product formations under oxygen limitation allow lower agitation rate, less aeration and thus less energy consumption, increasing the competitiveness of the next generation industrial biotechnology (NGIB) based on halophiles (Chen and Jiang, 2018; de las Heras et al., 2016).

This study aims to investigate and then engineer the redox potential of *H. bluephagenesis* to achieve better cell growth and PHA production.

2. Materials and methods

2.1. Strains and media

The bacterium used in this study was *Halomonas bluephagenesis* TD01 (NCBI: txid999141), *E. coli* JM109 and *E. coli* S17-1. *H. bluephagenesis* was cultured in a LB60 medium containing 60 g/L NaCl, *E. coli* in a normal LB medium, for enzymatic

assays and NADH/NAD^+ measurements; 2 g/L acetic acid was added into LB60 medium to verify the influence on redox states if required. DNA uptake via electroporation or chemical transformation are not possible for *H. bluephagenesis*, only conjugation with the help of *E. coli* S17-1 was proven practical for DNA transformation to *H. bluephagenesis*. Strains, plasmids and oligonucleotides used in this study are described in Table S1. Gibson assembly was used for plasmid constructions (Gibson et al., 2009) except for gRNA ligations based on BsaI and T4 DNA ligase (NEB, USA), complementary experiment of electron transfer flavoproteins subunit β encoded by gene *etf*-x-β based on blunt-end ligation via T4 PNK (NEB, USA) and T4 DNA ligase. Plasmids were verified via colony PCR and DNA sequencing. Antibiotics and their concentrations were prepared as followings (μg/mL): 50 kanamycin, 25 chloramphenicol, 100 ampicillin and 50 spectinomycin. Shake flask cultivation of *H. bluephagenesis* was carried out in modified mineral medium (MM60) consisting of 0.1% Urea, 0.02% $MgSO_4$, 1.0% $Na_2HPO_4 \cdot 12H_2O$, 0.15% KH_2PO_4, 1 g/L yeast extract, 60 g/L NaCl and 30 g/L glucose, any other modification will be indicated separately. The pH of the MM60 was adjusted to 8.5. Shake flask cultivations of *E. coli* were conducted in a mineral medium consisting of 0.1% $(NH_4)_2SO_4$, 0.02% $MgSO_4$, 1.0% $Na_2HPO_4 \cdot 12H_2O$, 0.15% KH_2PO_4, 1 g/L yeast extract and 30 g/L glucose. All chemicals were purchased from Sinopharm Chemical Reagent Co. (China) and Sigma-Aldrich (USA).

2.2. Gene knockout and recover experiment

All genes were knocked out via CRISPR/Cas9 method (Qin et al., 2018). The gRNA sequences are listed in Table S3. As cell growth was very poor in liquid cultures with glycine betaine (GB) or dimethylglycine (DMG) as a sole carbon source, growth of *H. bluephagenesis* on these sole carbon sources were conducted on plates as described (Haslinger and Prather, 2017; Rand et al., 2017). All the primers and plasmids sequences are listed in the supplementary files (Table S2).

2.3. Specific enzymatic assay

2.3.1. Cell cultivation and reagents preparation

The specific acetoacetyl-CoA reductase (PhaB or AAR) activities in cells of wild type *E. coli* JM109, *E. coli* JM109 containing plasmid pBHR68 encoding PHA synthesis operon *pha*CAB$^{C.\ necator}$ cloned from *C. necator*, *H. bluephagenesis* strains TD01 and TD-Δ*pha*B were assayed: *E. coli* strains were cultivated in LB medium, 100 μg/mL ampicillin were added to maintain stability of pBHR68 plasmid when necessary, and *H. bluephagenesis* strains were also cultivated in LB60 medium containing 60 g/L NaCl. Cells were harvested during the exponential phase via centrifugation under 2500 g, 4 °C for 10 minutes. Resultant pellets were washed via their suspension in 10% of the original culture volume using ice-cold Buffer A containing 50 mM Tris, 100 mM NaCl, 5 mM $MgCl_2$ and 5 % (v/v) glycerol at pH 8, followed by centrifugation again under 2500 g, 4 °C for 5 minutes. For cell-free extracts preparation, the sedimented pellets were re-suspended in 10% of the original culture volume using ice-cold buffer A supplemented with 2 mM DL-dithiothreitol. Cells were broken under sonication on ice to avoid over-heating. Cell-free extracts were obtained from the supernatants after centrifugation for 45 minutes at 4 °C under 15000 g.

Specific acetoacetyl-CoA reductase (AAR, or PhaB) activities in a purified form from *H. bluephagenesis* TD01 (tdPhaB) and *C. necator* H16 (cnPhaB) were assayed. The genes *pha*B^{td} and *pha*B^{cn} were PCR from the genome of *H. bluephagenesis* TD01 and plasmid pBHR68, respectively. They were subcloned to the vector pET28a (+). The sequenced plasmids were transformed to *E. coli* BL21 (DE3) for expression. Recombinant cells were cultivated to OD_{600} 0.6, followed by addition of IPTG to a final concentration of 1mM to induce plasmid expression. After 5 hours, Cells were collected via centrifugation under 2500 g, 4 °C for 10 minutes, the

sedimented pellets were treated based on the instructions of the His-tag Protein Purification Kit (P2226, Beyotime, China).

The substrates were freshly prepared by dissolving them in Buffer A. Concentrations of the resultant solutions were determined using VarioskanFlash plate reader (Version 4.00.53, Thermo Scientific, USA), using apparent molar extinction coefficients obtained under conditions similar to ours, such as ε^{app} at 340 nm for NAD(P)H = 6220 M^{-1} cm^{-1}; for acetoacetyl-CoA at 310 nm, ε^{app} = 11000 M^{-1} cm^{-1} (Stern, 1956).

2.3.2. NADH or NADPH assays

The reactions using NADH or NADPH as cofactors were studied in Buffer A at 30 °C. The concentrations of acetoacetyl-CoA and cofactors were 70 and 200 μM, respectively. All spectrophotometric studies were performed in a VarioskanFlash plate reader (Version 4.00.53) controlled by SkanIt Software 2.4.5 RE, correcting the path lengths to consider the heights of the liquid columns in that the reactions occurred. To estimate initial reaction rates, pseudo-linear temporal changes of the absorbance were considered within the time frame in which less than 5 % of the substrates were consumed. Concentrations of protein in the cell-free crude extracts and purified enzymes were assayed using the Bradford protein assay reagent (Bio-Rad) based on bovine serum albumin (Bio-Rad) as the standard (Bradford, 1976). The final concentrations of purified enzymes were adjusted to 0.5-1 nM during the assays.

2.3.3. Assays of PhaB activity

Both acetoacetyl-CoA and its reduced cofactor are consumed stoichiometrically during the reactions detectable at 340 nm. Therefore, to calculate the PhaB or AAR activity, consumptions of acetoacetyl-CoA and NAD(P)H were monitored via absorbance changes at 340 nm employed the following equation (Stern, 1956):

$$\varepsilon^{340}_{\mathrm{AcAcCoA}} = \mathrm{Abs}^{340}_{\mathrm{AcAcCoA}} * \frac{\varepsilon^{310}_{\mathrm{AcAcCoA}}}{\mathrm{Abs}^{310}_{\mathrm{AcAcCoA}}}$$

2.4. Measurements of the cellular concentrations of NADH and NAD^+

E. coli strains were cultivated in LB medium, 100 μg/mL ampicillin were added to maintain stability of pBHR68 plasmid when necessary, and *H. bluephagenesis* strains were cultivated in LB60 medium containing 60 g/L NaCl. All the cells were harvested during the exponential phase via centrifugation under 2500 g at 4 °C for 10 minutes. Then the cell concentrations were adjusted to OD_{600} = 0.6 under dilution. 300 μL cell cultures normalized to similar cell numbers were collected from each sample, followed by twice washing using ice-cold PBS at pH 7.4. The concentrations of NADH and NAD+ were measured respectively, using the Kit E2ND-100 purchased from Bioassay Systems (USA), and the NAD+/NADH ratio was calculated based on the resulting concentrations. All the operations were strictly conducted based on instructions of the NAD^+/NADH Assay Kit E2ND-100.

2.5. PHA production in shake flasks or bioreactors

H. bluephagenesis was cultured from single colony in 100 mL shake flasks containing 20 mL LB60 medium at 37 °C for 12-16 h as a primary seed culture. Subsequently, 200 μL primary seed culture was inoculated into a 20 mL LB60 medium as the secondary seed culture. After 8-10 h when the OD_{600} reached approximately 4, 2.5 mL of the resulting culture were inoculated into 50 mL modified MM60 in a 500 mL shake flask, acetate and antibiotics were optional, the initial pH was adjusted to 9. The cells were cultivated at 37 °C for 48 h at 200 rpm on a rotary shaker (HNY-2112B, Tianjin Honor Instrument Co., Ltd, Tianjin, China).

The fed-batch fermentation of *H. bluephagenesis* was carried out in a 7.5 L NBS bioreactor (NBS, BioFlo115, New Jersey, USA) containing 3 L modified mineral medium (MM60) consisting of 0.1% Urea, 0.02% $MgSO_4$, 1.0% $Na_2HPO_4 \cdot 12H_2O$, 0.15% KH_2PO_4, 1 g/L yeast extract, 60 g/L NaCl and 20 g/L glucose. The pH of the culture medium was adjusted to 8.5 by addition of an aqueous solution of 5 M NaOH. The aeration was maintained at 1 *vvm* throughout the fermentation process. The

agitation speed started from 300 rpm, and was monitored to maintain the dissolved oxygen tension above 20% from 0 to 6 h by increasing 100 rpm each time interval, the agitation speed was set at the maximum 800 rpm after 6 h (Fig. S1). The glucose concentration was monitored off-line to maintain at around 10 g/L during the cell growth process using an aqueous solution of 600 g/L glucose. A total of 12 g urea was supplemented intermittently to the fermentor vessel during the initial 6 -28 h for a higher cell density growth.

2.6. Analytical methods

2.6.1. PHA assays via gas chromatography (GC)

The bacterial cells were harvested after 48 h via centrifugation at 10,000 g for 10 min, followed by washing once with 20 mL of deionized water. Cell dry weights (CDW) were determined after vacuum lyophilization (LGJ-10C, Beijing Sihuan Scientific Instrument Factory Co., Ltd, China). The PHB contents were analyzed using gas chromatography (GC-2014, SHIMADZU, Japan) after methanolysis of lyophilized cells in chloroform as described (Tan et al., 2011).

2.6.2. Analyses of residual glucose, acetate and secreted pyruvate

The concentrations of secreted extracellular pyruvate and residual glucose were analyzed using liquid chromatography/mass spectrometry (LC/MS, Q Exactive Orbitrap, Thermo, CA, USA). The samples were centrifuged at 4700 g for 30 minutes to obtain the supernatants (Multifuge X3R, Thermo Scientific, USA). 100 μL of a supernatant were added to 400 μL of methanol that had been stored at -80^{o}C for more than 12 h. The mixture of supernatant and methyl alcohol was then maintained at -80 ^{o}C for 2 h followed by centrifugation at 10000 g for 20 min to obtain the supernatant for analysis using Q Exactive Orbitrap. 1 μL supernatant was loaded onto a normal phase chromatography column. Then, the sample was eluted for Orbitrap mass spectrometer with 100% H_2O containing 5 mM ammonium acetate as eluent. The data

with mass ranges of m/z 80-1200 were acquired at negative ion mode with data dependent MS acquisition. The full scan and fragment spectra were collected with resolution of 70,000 and 17,500, respectively. The source parameters are: spray voltage: 3000 v; capillary temperature: 320 ^{o}C; heater temperature: 300 ^{o}C; sheath gas flow rate: 35; auxiliary gas flow rate: 10.

The residual acetate in the supernatants was analyzed using a high-performance liquid chromatography (HPLC) (LC-20A, SHIMADZU, Japan) equipped with an ion exchange column (BioRad, Aminexs HPX-87H, 7.8×300 mm^2) and a refractive index detector (RID-10A, SHIMADZU, Japan). A mobile phase of 5 mM H_2SO_4 at a 0.6 mL/min flow rate was used. The working temperature of the ion exchange column was 40 ^{o}C.

2.7. Transmission electron microscopy (TEM) observation

The bacterial cells were harvested by centrifugation at 5,000 g for 3 min, washed three times with PBS (phosphate buffer saline with a pH 7.2). Subsequently, the cells were fixed with 2% glutaraldehyde (pH 7.2) at room temperature for 2 h and washed again as described above. The cells were prepared for scanning or transmission electron microscopy as described previously (Denner et al., 1994).

3. Results

3.1. PHB accumulation by *H. bluephagenesis* TD01 under oxygen limitation

H. bluephagenesis TD01 was found to accumulate more PHB under oxygen limitation compared with *E. coli* JM109 harboring *pha*CAB operon of *C. necator* (*pha*CAB$^{C.\ necator}$) during growth in shake flask (Fig. 1A) and fed-batch bioreactor (Fig. 1B), respectively. Previously, Tolosa et al. proved that the shaker speed significantly influenced the dissolved oxygen in shake flasks, and oxygen limitation occurred at a lower shaker speed (Tolosa et al., 2002). Under lower shaker speed of 200 rpm shake flask studies, *H. bluephagenesis* and the recombinant *E. coli* were

grown to 11.3 g/L CDW with 86% PHB and 6.4 g/L CDW with 65% PHB, respectively, compared to only 5.4 g/L CDW with 58% PHB and 6.0 g/L CDW with 60% PHB for both strains grown under higher aeration of 300 rpm, respectively (Fig. 1A, Table S4). The aeration intensity affects very little on growth and PHB accumulation by recombinant *E. coli*. In contrast, the lower aeration both increased PHB accumulation and correlated to a higher CDW in *H. bluephagenesis* (Fig. 1A Table S4).

During the fed-batch fermentation process conducted in a 7.5 L fermentor, oxygen limitation occurred at 8 h of the growth process (Fig. 1B). The PHB accumulation can be observed to rapidly increase and also maintained increasing from 8 h to 48 h during the entire oxygen limitation incubation, while the non-PHB residual biomass in turn decreased slowly, possibly due to the secretion of pyruvate during the fermentation process (Ye et al., 2018b). Under agitations of 800 rpm, 280 rpm and 170 rpm, or at constant aeration rates of 1 *vvm*, 1 *vvm*, 0.85 *vvm* for fermentors with sizes of 7.5 L, 1-m^3 and 5-m^3, respectively, *H. bluephagenesis* could be grown to over 90 g/L CDW containing at least 74% PHA (Ye et al., 2018b). The PHA productivity of *H. bluephagenesis* could reach 1.85 g/L h under oxygen limitation conditions, which was much higher than that of *A. beijierinckii* (0.83 g/L h), and even comparable to that of *C. necator* (2.63 g/L h) under pure oxygen aeration (Kim et al., 2004; Preusting et al., 1993; Soo et al., 1994). These results highly recommend that PHB synthesis by *H. bluephagenesis* is a fermentation process rather than an anabolism one, and thus, PHB synthesis by *H. bluephagenesis* should be NADH dependent instead of NADPH dependent.

3.2. Identification and activity assay of the major PhaB in *H. bluephagenesis* TD01

The PHB accumulation under anabolism or fermentation depends on the preferences of cofactor utilization by acetoacetyl-CoA reductase (PhaB or AAR). The

putative PhaB of *H. bluephagenesis* TD01 (WP_009724067.1, tdPhaB) was identified using bioinformatics analysis to have the highest identity (55% identity and 97% query cover) to that of *C. necator* (cnPhaB, PDB: 3VZP). In order to confirm the function of the putative PhaB, tdPhaB was deleted via CRISPR/Cas9 method, shake flask studies showed that *H. bluephagenesis* TD-Δ*pha*B could only be grown to 3 g/L CDW containing only 15% PHB compared with 10.5 g/L CDW accumulating 80% PHB by the wild type *H. bluephagenesis* TD01 (Fig. 2A, Table S4).

Phylogenetic analyses were conducted based on the PhaB amino acid sequences and the 16s ribosomal RNA sequences of *H. bluephagenesis*, *Cupriavidus necator*, *Pseudomonas putida*, *Azotobacter beijerinckii* and *Allochromation vinosum*, respectively. Interestingly, the four strains including *H. bluephagenesis*, *P. putida*, *A. beijerinckii* and *A. vinosum* are closer in taxonomy compared with *C. necator* according to the 16s rRNA sequences analysis (Fig. S2A). However, the PhaBs of *H. bluephagenesis* and *A. vinosum* are less similar to the other three species, especially, the PhaB of *H. bluephagenesis* is most distinctive from all the other species (Fig. S2B).

The sequence analysis on tdPhaB, cnPhaB and PhaB of *A. vinosum* (avPhaB) reveals significant differences on their NAD(P)(H) binding regions (Fig. 3A). The only difference between NAD(H) and NADP(H) is the extra phosphate of NADP(H). The three amino acids (Gly35, Ser38 and Arg40) have been proven to interact with 3'-phosphate in cnPhaB, while all the three amino acids are absent in the NAD(P)(H) binding domain of tdPhaB and avPhaB (Fig. 3A and B) (Kim et al., 2014; Matsumoto et al., 2013). Instead, a glutamate was found in this domain in tdPhaB and avPhaB (Fig. 3B), which has acidic residue perfectly for hydrogen bond formation to hydroxyl groups on the adenine ribose of NAD(H) (Suhadolnik et al., 1977).

In order to confirm the utilization of NADH cofactor during PHB synthesis by *H. bluephagenesis* TD01, specific enzymatic activity assay was conducted using crude cell extract of *E. coli* JM109 harboring the cnPhaB, *H. bluephagenesis* strains TD01,

TD-Δ*pha*B, and wild type *E. coli* JM109 as a control. As a result, *H. bluephagenesis* TD01 was found to have significant preference to NADH over NADPH, with NADH/NADPH consumption ratio of more than 26, the most preferential ratio for NADH ever reported (Fig. 2B, Table S5), the previous highest ratio was 4.7 reported in *A. vinosum* (Liebergesell and Steinbuchel, 1992). Preference of NADH for PHB synthesis enables *H. bluephagenesis* TD01 to accumulate PHB under oxygen-limited condition via fermentation directly from acetyl-CoA.

We also purified the cnPhaB and tdPhaB using His-Tag (Fig. S3). The enzymatic assays based on the purified proteins clearly support our conclusion that tdPhaB prefers NADH instead of NADPH during the reduction of acetoacetyl-CoA (Table S6).

3.3. Assays of cellular NADH/NAD^+ ratios in *H. bluephagenesis*

Based on the fact that PHB accumulation by *H. bluephagenesis* TD01 is mainly a fermentation process consuming NADH under oxygen limitation condition, NADH/NAD^+ ratio becomes very important to channel the acetyl-CoA flux to PHB synthesis (Anderson and Dawes, 1990; de las Heras et al., 2016). The NADH/NAD^+ ratio varies from species to species, it is usually less than 1, with the only exception of *Pseudomonas aeruginosa* (Farhana et al., 2010; Wimpenny and Firth, 1972), which contains phenazine as the electron receptor under hypoxic condition, this is similar to the acetoacetyl-CoA reduction during PHB synthesis by *H. bluephagenesis* TD01 (Farhana et al., 2010).

H. bluephagenesis TD01 grown in LB showed a NADH/NAD^+ ratio of more than 1.5 compared to only less than 0.2 of *E. coli* (Fig. 4A and B), revealing the reason of high PHB accumulation under oxygen limitation (Anderson and Dawes, 1990). However, abnormal increase on NADH could inhibit pyruvate metabolism (Fig. 6B). Although NADH could be consumed for PHB synthesis, one NADH is left when two pyruvates are converted to one 3HB-CoA (Fig. 5B). Excessive NADH is found

especially under high cell density growth when oxygen becomes severely limited, inhibiting pyruvate metabolism, thus wasting carbon source (Fig. 6B).

3.4. Effects of acetic acid on PHB accumulation

The acetate over-production was reported in *E. coli* K-12 grown on excess glucose even under aerobic conditions (Andersen and von Meyenburg, 1980; Meyer et al., 1984; Vemuri et al., 2006). The acetate formation can be completely eliminated via oxidation of excess NADH, however, more carbon flux will flow to CO_2 resulting in substrate waste (Vemuri et al., 2006). However, acetate has seldom been detected in cultures *H. bluephagenesis* (Ouyang et al., 2018). The reductive metabolism of acetate to ethanol using surplus NADH was observed in some *Clostridium* species (Wei et al., 2013). It is thus expected that surplus NADH generated from glycolysis and pyruvate metabolism in *H. bluephagenesis* TD01 could provide the reducing equivalent for acetate reduction to generate more acetyl-CoA for PHB synthesis under oxygen limitation condition (Fig. 5A).

Acetate is a cost-effective carbon source that can be produced from carbon dioxide and hydrolysis or pyrolysis of lignocellulosic biomass like corn stover (Hu et al., 2016; Wei et al., 2013; Zhang, 2008). The acetate utilization genes have been identified in *H. bluephagenesis* TD01 via NCBI database, including acetyl-coenzyme A synthetase (*acs*A, GenBank: EGP21698.1), acetate kinase (*ack*A; GenBank: EGP18271.1, EGP20583.1) and phosphate acetyltransferase (*pta*, GenBank: EGP20582.1). The NADH/NAD^+ ratio was observed to decrease accompanied by increasing NAD^+ in the presence of acetic acid (Fig. 4A and B), more NAD^+ could reduce inhibition of pyruvate metabolism, thus enhance PHB accumulation (Fig. 6, Table S4).

The amount of acetyl-CoA flux into PHB synthesis was calculated based of the average PHB content of standard shake flask data. Approximately 9 g/L PHB are produced from 30 g/L glucose: 0.1 mol/L 3HB-CoA is generated from 0.2 mol/L

pyruvate, leaving 0.1 mol/L NADH unconsumed behind. Theoretically, the highest concentration of 12 g/L acetic acid could be converted to PHB synthesis if all the remaining NADH were consumed regardless of the ATP consumption during acetate transferring to acetyl-CoA (Fig. 5).

The concentration gradients of acetic acid (g/L) 3, 6, 9 and 12 were co-fed with 30 g/L glucose for growth of *H. bluephagenesis* TD01, respectively (Fig. 6A). The 3 g/L acetic acid increased 20% CDW and 5% PHB content without pyruvate formation and residual glucose, and the 6 g/L acetate led to the highest CDW and PHB accumulation (Fig. 6A, Table S4), while 0.5 g/L residual glucose together with 0.2 g/L pyruvate were found in the culture (Fig. 6B), and the residual acetate was observed below 0.1 g/L. Only at 12 g/L acetate, 4 g/L acetate remained unconsumed. More than 9 g/L acetate seemed to inhibit cell growth. Advantages of additional acetate over pyruvate were visible from shake flask studies: 30 g/L glucose were an optimal concentration, additional acetic acid enhanced growth and PHB accumulation, extra pyruvate inhibited cell growth and PHB synthesis (Fig. 6C, Table S4).

3.5. Deleting electron transfer flavoprotein reduced redox state of *H. bluephagenesis*

Disruption on NADH utilization pathway, or NADH dependent respiratory chain, was reported to increase the NADH/NAD^+ ratio for enhanced PHB accumulation by *A. beijerinckii* (Page and Knosp, 1989). Two sets of electron transfer flavoproteins (ETF) and one ETF- ubiquinone oxidoreduacase (ETF-QO, or electron transfer flavoprotein dehydrogenase) in the genome of *H. bluephagenesis* TD01 via bioinformatics analysis using the UNIPROT database. Both ETFs have two subunits α and β under the same operon, and *etf*-qo locates in the *etf*-1 operon. During the protein sequence analysis, one set ETF-1 (NCBI Reference Sequence: WP_009722059.1, WP_009722058.1) is highly conserved, with 99% query cover and more than 60% identity of both subunits to the ETF of *Homo sapiens* (GenBank: SJM32114.1, SJM32113.1). They are

supposed to shuttle electrons from NADH dependent dehydrogenase to the ETF-QO (GenBank: AAB24227.1) in fatty acid and amino acid metabolism. The ETF-QO is also conserved with 97% query cover and 51% identity to the ETF-QO of *Sus scrofa* (UNIPROT: P55931), which was reported to link oxidation of fatty acids and some amino acids to the respiratory chain (Zhang et al., 2006); the other set with unclear function (named as ETF-X, NCBI Reference Sequence: WP_009724031.1, WP_009724032.1) has relatively low identity but is also conserved in the FAD binding sites.

The comparative genomic analysis of *H. bluephagenesis* TD01 and *Pseudomonas aeruginosa* PA14 based on the annotation in UNIPROT together with KEGG databases, indicates that the *etf*-x loci are very similar across these two distinctive species (Fig. 7A). Particularly, most genes near *etf*-x loci have been proven related to glycine betaine (GB) metabolism in *P. aeruginosa* PA14 including *gbc*AB and *dgc*AB (Wargo, 2013; Wargo et al., 2008) (Fig. 7B). However, the relationship between *etf*-x and GB metabolism related genes has never been discussed in all organisms. We further used STRING database to systematically evaluate the correlations between *etf*-x and *etf*-qo, *etf*-x and GB metabolism related genes, respectively. The neighborhood score, namely, neighborhood correlation between genes on the chromosome, and total score (comprehensive functional) were used for the evaluation (Fig. 7C). The results strongly suggest that ETF-X act as the electron shuttle between GB metabolism and the conserved ETF-QO, which transfers the reducing equivalent to the respiratory chain.

In order to confirm the function of *etf*-x genes, *etf*-x-α and *etf*-x-β was deleted in *H. bluephagenesis* strains TD01 via CRISPR/Cas9 method, resulting in *H. bluephagenesis* strains TD-Δα and TD-Δβ (Fig. 8A), respectively. *H. bluephagenesis* strains TD01, TD-Δα and TD-Δβ with empty vector pSEVA321 as well as complementary plasmids pSEVA321-α and pSEVA321-β were grown on Petri dishes containing modified mineral medium (MM60) consisting of 0.1% Urea, 0.02%

$MgSO_4$, 1.0% $Na_2HPO_4 \cdot 12H_2O$, 0.15% KH_2PO_4, 60 g/L NaCl and 2% agar, with GB, dimethylglycine (DMG) and glucose as the sole carbon sources, respectively. *H. bluephagenesis* strains TD-Δα and TD-Δβ with empty vector were grown very poorly on Petri dishes with DMG or GB as the sole carbon source while complementary experiments showed robust growth (Table 1). All the details are available (Fig. S4). These results together with the bioinformatics analysis provide strong evidences that ETF-X plays the electron shuttling role between GB metabolism and ETF-QO.

The NADH/NAD^+ ratio was higher in *H. bluephagenesis* TD-Δβ than that of *H. bluephagenesis* TD01, while the NADH and NAD^+ pool stayed almost the same (Fig. 4). The genetic disruption of *etf*-x-β has limited influence on cell growth in LB medium (Fig. S5). The shake flask studies on *H. bluephagenesis* strains TD-Δβ and of TD01 conducted in MMG medium added with acetate of concentration gradients, respectively, revealed an ultra-high PHB content of more than 94% accumulated by *H. bluephagenesis* TD-Δβ at 3 g/L acetate (Fig. 8B, Table S4), enlarged cells fully filled with larger PHB granules (Fig. 8C).

3.6. Controllable acetyl-CoA flux via adjusting redox state for PHBV and P34HB synthesis

The copolymers P34HB and PHBV are better materials compared to homopolymer PHB (Byrom, 1987; Choi and Lee, 1999; Saito and Doi, 1994). However, the 3HV or 4HB fractions in their copolymers are difficult to increase using glucose as the sole carbon source in *H. bluephagenesis* strains (Ye et al., 2018a; Yin et al., 2015). The PHB monomer, 3HB, is synthesized from acetyl-CoA via two steps without oxygen consumption, can be considered as NADH based fermentation. Whereas other PHA monomers, such as hydroxyvalerate (3HV) and 4-hydroxybutyrate (4HB), mainly derived from intermediates of the TCA cycle and glyoxylate shunt (Fig. 5A). Previously, disruption of the glyoxylate shunt by knocking out two genes *aceBA* led to dramatic decrease in 4HB synthesis. A mutated

citrate synthase was employed to avoid enzyme inhibition by NADH, resulting in a higher 4HB percentage in P34HB (Choi et al., 2016). Thus, we reason that the 4HB and 3HV fractions in their copolymers depend on the acetyl-CoA flux into the TCA cycle and glyoxylate shunt, which could be controlled by systematically modulating the redox state, namely, the NADH/NAD^+ ratio (Fig. 4A). For P34HB and PHBV synthesis by *H. bluephagenesis* TD01, acetyl-CoA can be regarded as the crossroad of anabolism and fermentation, and the "traffic police" should be NADH and NAD^+ (Fig. 5A).

The concentration gradients of acetate of 2, 4 and 6 g/L were co-fed with 30 g/L glucose to culture of H. bluephagenesis TD08AB containing a 3HV synthesis pathway (Fu et al., 2014) and *H. bluephagenesis* TDΔgabD2-D2 containing a 4HB synthesis pathway (Ye et al., 2018a), respectively. The presence of 2 g/L acetic acid increased 3HV ratio in the PHBV copolymers from 4.2% to 8.4%. While 4 g/L acetate in the medium increased 4HB ratio in the P34HB from 7.9% to 12.0%, compared to culture without acetate, respectively (Fig. 9A and B, Table S4). Too higher an acetate concentration of over 4 g/L could not bring benefits for cell growth and PHA accumulation (Fig. 9A and B, Table S4).

4. Discussion and conclusion

Halomonas bluephagenesis, as the first bacterial strain successfully developed as a platform for the next generation industrial biotechnology (NGIB), allows productions of PHA, small molecules and proteins to be conducted under open and continuous conditions (Chen and Jiang 2018; Ye et al., 2018b). A continuous cell growth was observed to be associated with PHA accumulation under oxygen limitation, the mechanism was unclear (Ye et al 2018b). For the first time in this study, it was clearly found that *H. bluephagenesis* was able to grow at lower aeration and accumulate 30% more PHB compared with recombinant facultative aerobic *E. coli* harboring PHA synthesis operon. Unlike *E. coli*, a higher aeration negatively affected

cell growth and PHB synthesis (Fig. 1A). A fed-batch fermentation study convincingly showed that PHB rapid accumulation was induced by oxygen limitation (Fig. 1B), the PHB content maintained continuously increasing trend throughout the entire 48 growth period, even though the cells were constantly under oxygen limitation pressure after 12 h of growth (Fig. 1B). This is a very beneficial growth pattern for many high cell density growth processes that have to experience oxygen limitation. In fact, low aeration reduces energy demands by the air compressors, thus increasing the process efficiencies.

It was very fortunate to discover that acetoacetyl-CoA reductase (PhaB), a key enzyme for PHA biosynthesis, is a NADH dependent enzyme rather than a NADPH dependent one (Fig. 2). So far, only three bacteria including *Allochromatium vinosum*, *Azotobacter beijierinckii* and *H. bluephagenesis* have been reported to have a NADH dependent PhaB (Fig. 3A). Since NADH can be generated from fermentation under oxygen limitation or even anaerobic growth, the NADH dependent PHB synthesis process in *H. bluephagenesis* has become a fermentation process rather than an oxygen dependent and thus NADPH dependent one. This is the mechanism behind oxygen limitation induced PHA synthesis observed in our studies (Ye et al., 2018b).

Since PhaB of *H. bluephagenesis* is depending on NADH content for PHA synthesis, the sources of NADH and its consumption pathways were investigated (Fig. 5A). It was found that pyruvate metabolism to acetyl-CoA, glycine betaine to dimethyl glycine and dimethyl glycine to methyl glycine can supply NADH to its pool (Fig. 5A), while some NADH was consumed by respiratory chain. There is possibility to *in vitro* and *in vivo* engineering the NADH/NAD^+ ratio for more PHA synthesis (Fig. 5).

On the other hand, the fermentative consumption of NADH for PHB synthesis could not consume all NADH (Fig. 5B), leading to inhibition on pyruvate metabolism and TCA cycle (Figs. 5A, 6B). Luckily, acetate utilization genes have been found in *H. bluephagenesis* TD01 via the NCBI database, including acetyl-coenzyme A

synthetase, acetate kinase and phosphate acetyltransferase, they allow acetate to be converted to acetyl-CoA by consuming NADH (Fig. 4). The increasing amount of acetyl-CoA supplies more acetyl-CoA as a substrate both for PHA synthesis and for TCA cycle, improving not only PHA synthesis but also cell growth. The presence of less than 6 g/L acetic acid effectively increased cell growth and PHB accumulation (Fig. 6).

The disruption of NADH utilization pathway, namely, NADH dependent respiratory chain can be explored to increase the $NADH/NAD^+$ ratio to enhance the PHA accumulation. Two sets of electron transfer flavoproteins (ETF) and one ETF-oxidoreduacase (ETF-QO) have been predicted in *H. bluephagenesis* TD01 via the UNIPROT database. Both *etf*s have two subunits α and β in the same operon, and *etf*-qo locates in the *etf*-1 operon. When subunit *etf*-x-β was deleted, growth of the resulting *H. bluephagenesis* TD-Δβ was not affected, yet the ability to accumulate PHB was significantly enhanced from 85% of the wild type to 94% by the *etf*-x-β deleted *H. bluephagenesis* TD-Δβ in the presence of acetic acid (Fig. 9). It is estimated that $NADH/NAD^+$ ratio was further increased in *H. bluephagenesis* TD-Δβ, resulting in more PHB accumulation. Thus, the manipulation on NADH utilization pathway serves as an *in vivo* way to improve $NADH/NAD^+$ ratio for higher PHB accumulation.

The addition of acetic acid acetate improves the TCA cycle as the inhibition of citrate synthase can be reduced at a lower $NADH/NAD^+$ ratio. The monomers for PHA synthesis, especially 3-hydroxyvalerate (3HV) and 4-hydroxybytyrate (4HB) that are derived from TCA cycle, are increased in flux for PHBV and P34HB synthesis. Thus, acetic acid can be used as an *in vitro* tool to systematically modulate the $NADH/NAD^+$ ratio, leading to improved PHA synthesis and enhanced non-3HB copolymer monomer ratio (Fig. 9).

For the first time, our study uncovers the preference of NADH cofactor during PHA accumulation by *H. bluephagenesis* TD01. The pyruvate metabolism would be

inhibited by the over reductive condition. The acetate reduction to 3HB-CoA helps consume NADH thus lower NADH/NAD^+ ratio. In this case, the acetate functions as *in vitro* redox regulator.

In conclusion, the successful engineering on redox potential of *H. bluephagenesis* using acetic acid as an *in vitro* tool and disruption on non-essential respiratory chain as an *in vivo* method led to enhanced PHA accumulation and controllable monomer ratios in copolymers under oxygen limitation, which is a dream process for reduced energy consumption and reduced scale-up complexity. The NADH dependent PHA accumulation process provides additional energy saving advantage for *H. bluephagenesis* as the next generation industrial biotechnology platform organism.

Conflict of interest

The authors declare no financial or commercial conflict of interest.

Acknowledgements

We are grateful to the Center of Biomedical Analysis at Tsinghua University, Beijing, China, for the TEM and LC/MS analysis. We are also grateful for the donation of SEVA plasmids by Prof. Victor de Lorenzo of CSIC, Spain. We are also grateful for the donation of pBHR68 plasmid by Prof. Dr. Uwe Sauer of ETH, Switzerland. This research was financially supported by a grant from Ministry of Sciences and Technology (Grant No. 2016YFB0302500), and grants from National Natural Science Foundation of China (Grant No. 31430003). Tsinghua President Fund also supported this project (Grant No. 2015THZ10). The contribution of Karel Olavarria was supported by SIAM Gravitation grant (024.002.002) of the Netherlands Ministry of Education, Culture and Science (OCW) and the Netherlands Organisation for Scientific Research (NWO).

Appendix A. Supplementary material

Supplementary data associated with this article can be found in the online version at

References

Andersen, K. B., von Meyenburg, K., 1980. Are growth rates of *Escherichia coli* in batch cultures limited by respiration? J Bacteriol. 144, 114-123.

Anderson, A. J., Dawes, E. A., 1990. Occurrence, metabolism, metabolic role, and industrial uses of bacterial polyhydroxyalkanoates. Microbiol Rev. 54, 450-472.

Beckers, V., Poblete-Castro, I., Tomasch, J., & Wittmann, C., 2016. Integrated analysis of gene expression and metabolic fluxes in PHA-producing *Pseudomonas putida* grown on glycerol. Microb Cell Fact. 15(1), 73.

Borrero-de Acuña, J. M., Bielecka, A., Häussler, S., Schobert, M., Jahn, M., Wittmann, C., Jahn, D., Poblete-Castro, I., 2014. Production of medium chain length polyhydroxyalkanoate in metabolic flux optimized *Pseudomonas putida*. Microb Cell Fact. 13**,** 88.

Bradford, M. M., 1976. A rapid and sensitive method for the quantitation of microgram quantities of protein utilizing the principle of protein-dye binding. Anal Biochem. 72, 248-254.

Byrom, D., 1987. Polymer synthesis by microorganisms: technology and economics. Trends Biotechnol. 5, 246-250.

Chen, G. Q., Jiang, X. R., 2018. Next generation industrial biotechnology based on extremophilic bacteria. Curr Opin Biotechnol. 50, 94-100.

Chen, X., Yin, J., Ye, J., Zhang, H., Che, X., Ma, Y., Li, M., Wu, L. P., Chen, G. Q., 2017. Engineering *Halomonas bluephagenesis* TD01 for non-sterile production of poly(3-hydroxybutyrate-co-4-hydroxybutyrate). Bioresour Technol. 244, 534-541.

Choi, J.-i., Lee, S. Y., 1999. High-level production of poly(3-hydroxybutyrate-co-3-hydroxyvalerate) by fed-batch culture of recombinant *Escherichia coli*. Appl Environ Microbiol. 65, 4363-4368.

Choi, S., Kim, H. U., Kim, T. Y., Lee, S. Y., 2016. Systematic engineering of TCA cycle for optimal production of a four-carbon platform chemical 4-hydroxybutyric acid in *Escherichia coli*. Metab Eng. 38, 264-273.

de las Heras, A. M., Portugal-Nunes, D. J., Rizza, N., Sandström, A. G., Gorwa-Grauslund, M. F., 2016. Anaerobic poly-3-d-hydroxybutyrate production from xylose in recombinant *Saccharomyces cerevisiae* using a NADH-dependent acetoacetyl-CoA reductase. Microb Cell Fact. 15, 197.

Denner, E. B. M., McGenity, T. J., Busse, H.-J., Grant, W. D., Wanner, G., Stan-Lotter, H., 1994. *Halococcus salifodinae sp.* nov., an Archaeal isolate from an Austrian salt mine. Int J Syst Evol Microbiol. 44, 774-780.

Farhana, A., Guidry, L., Srivastava, A., Singh, A., Hondalus, M. K., Steyn, A. J. C., 2010. Reductive Stress in Microbes: Implications for Understanding *Mycobacterium tuberculosis* Disease and Persistence. In: Poole, R. K., (Ed.), Adv Microb Physiol. vol. 57. Academic Press, pp. 43-117.

Ferre-Guell, A., Winterburn, J. 2018. Biosynthesis and characterization of polyhydroxyalkanoates with controlled composition and microstructure. Biomacromolecules 19, 996-1005

Fu, X. Z., Tan, D., Aibaidula, G., Wu, Q., Chen, J. C., Chen, G. Q., 2014. Development of *Halomonas* TD01 as a host for open production of chemicals. Metab Eng. 23, 78-91.

Gibson, D. G., Young, L., Chuang, R.-Y., Venter, J. C., Hutchison Iii, C. A., Smith, H. O., 2009. Enzymatic assembly of DNA molecules up to several hundred kilobases. Nat Methods. 6, 343.

Haslinger, K., Prather, K. L. J., 2017. Pathway towards renewable chemicals. Nat Microbiol. 2, 1580-1581.

Hu, P., Chakraborty, S., Kumar, A., Woolston, B., Liu, H., Emerson, D., Stephanopoulos, G., 2016. Integrated bioprocess for conversion of gaseous substrates to liquids. Proc Natl Acad Sci U S A. 113, 3773-3778.

Ishizaki, A., Tanaka, K., 1990. Batch culture of *Alcaligenes eutrophus* ATCC 17697T using recycled gas closed circuit culture system. J Ferment Bioeng, 69(3), 170-174.

Ishizaki, A., Tanaka, K., 1991. Production of poly-β-hydroxybutyric acid from carbon dioxide by *Alcaligenes eutrophus* ATCC 17697T. J Ferment Bioeng, 71(4), 254-257.

Ishizaki, A., K. Tanaka., 1992. Production of PHB from carbon dioxide employing *Alcaligenes eutrophus* ATCC 17697T using a two stage culture system." The Abstracts of ISBP. Vol. 92.

Jackson, F. A., Dawes, E. A., 1976. Regulation of the Tricarboxylic Acid Cycle and Poly-β-hydroxybutyrate Metabolism in *Azotobacter beijerinckii* Grown under Nitrogen or Oxygen Limitation. Microbiology. 97, 303-312.

Kim, B. S., Lee, S. C., Lee, S. Y., Chang, H. N., Chang, Y. K., Woo, S. I., 2004. Production of poly(3-hydroxybutyric acid) by fed-batch culture of *Alcaligenes eutrophus* with glucose concentration control. Biotechnol Bioeng. 43, 892-898.

Kim, B. S., Lee, S. Y., Chang, H. N., 1992. Production of poly-β-hydroxybutyrate by fed-batch culture of recombinant *Escherichia coli*. Biotechnol Lett. 14, 811-816.

Kim, J., Chang, J. H., Kim, E.-J., Kim, K.-J., 2014. Crystal structure of (R)-3-hydroxybutyryl-CoA dehydrogenase PhaB from *Ralstonia eutropha*. Biochem Biophys Res Commun. 443, 783-788.

Koller, M., Marsalek, L., Dias, M. M. D. S., Braunegg, G. 2017. Producing microbial polyhydroxyalkanoate (PHA) biopolyesters in a sustainable manner. New Biotechnol. 37, 24-38

Kucera, D., Pernicova, I., Kovalcik, A., Koller, M., Mullerova, L., Sedlacek, P., Mravec, F., Nebesarova, J., Kalina, M., Marova, I., Krzyzanek, V., Obruca, S. 2018. Characterization of the promising poly(3-hydroxybutyrate) producing halophilic bacterium *Halomonas halophile*. Biores Technol. 256, 552-556

Le Meur, S., Zinn, M., Egli, T., Thony-Meyer, L., Ren, Q. 2014. Improved

productivity of poly(4-hydroxybutyrate) (P4HB) in recombinant *Escherichia coli* using glycerol as the growth substrate with fed-batch culture. Microb Cell Fact. 13:131

Lee, S. Y., 1996. Bacterial polyhydroxyalkanoates. Biotechnol Bioeng. 49, 1-14.

Matsumoto, K. i., Tanaka, Y., Watanabe, T., Motohashi, R., Ikeda, K., Tobitani, K., Yao, M., Tanaka, I., Taguchi, S., 2013. Directed evolution and structural analysis of NADPH-dependent acetoacetyl Co-enzyme A (Acetoacetyl-CoA) reductase from *Ralstonia eutropha* reveals two mutations responsible for enhanced kinetics. Appl Environ Microbiol. 79, 6134-6139.

Matthias, L., Alexander, S., 2005. Cloning and nucleotide sequences of genes relevant for biosynthesis of poly (3-hydroxybutyric acid) in *Chromatium vinosum* strain D. Eur J Biochem. 209, 135-150.

Meyer, H.-P., Leist, C., Fiechter, A., 1984. Acetate formation in continuous culture of *Escherichia coli* K12 D1 on defined and complex media. J Bacteriol. 1, 355-358.

Page, W. J., Knosp, O., 1989. Hyperproduction of poly-β-hydroxybutyrate during exponential growth of *Azotobacter vinelandii* UWD. Appl Environ Microbiol. 55, 1334-1339.

Poblete-Castro, I., Binger, D., Rodrigues, A., Becker, J., Dos Santos, V. A. M., & Wittmann, C., 2013. In-silico-driven metabolic engineering of *Pseudomonas putida* for enhanced production of poly-hydroxyalkanoates. Metab Eng. 15, 113-123.

Portugal-Nunes, D. J., Pawar, S. S., Liden, G., Gorwa-Grauslund, M. F. 2017. Effect of nitrogen availability on the poly-3-D-hydroxybutyrate accumulation by engineered *Saccharomyces cerevisiae*. AMB Express. DOI: 10.1186/s13568-017-0335-z

Preusting, H., van Houten, R., Hoefs, A., van Langenberghe Eddy, K., Favre-Bulle, O., Witholt, B., 1993. High cell density cultivation of *Pseudomonas oleovorans*: Growth and production of poly (3-hydroxyalkanoates) in two-liquid phase batch and fed-batch systems. Biotechnol Bioeng. 41, 550-556.

Qin, Q., Ling, C., Zhao, Y., Yang, T., Yin, J., Guo, Y., Chen, G. Q., 2018. CRISPR/Cas9 editing genome of extremophile *Halomonas spp*. Metab Eng. 47, 219-229.

Ouyang, P. F., Wang, H., Hajnal, I., Wu, Q., Guo, Y. Y., Chen, G. Q., 2018. Increasing oxygen availability for improving PHB production by *Halomonas*. Metab Eng. 45, 20-31

Rand, J. M., Pisithkul, T., Clark, R. L., Thiede, J. M., Mehrer, C. R., Agnew, D. E., Campbell, C. E., Markley, A. L., Price, M. N., Ray, J., Wetmore, K. M., Suh, Y., Arkin, A. P., Deutschbauer, A. M., Amador-Noguez, D., Pfleger, B. F., 2017. A metabolic pathway for catabolizing levulinic acid in bacteria. Nat Microbiol. 2, 1624-1634.

Ritchie, G. A. F., Senior, P. J., Dawes, E. A., 1971. The purification and characterization of acetoacetyl-coenzyme A reductase from *Azotobacter*

beijerinckii. Biochem J. 121, 309-316.

Saito, Y., Doi, Y., 1994. Microbial synthesis and properties of poly(3-hydroxybutyrate-co-4-hydroxybutyrate) in *Comamonas acidovorans*. Int J Biol Macromol. 16, 99-104.

San, K.-Y., Bennett, G. N., Berríos-Rivera, S. J., Vadali, R. V., Yang, Y.-T., Horton, E., Rudolph, F. B., Sariyar, B., Blackwood, K., 2002. Metabolic engineering through cofactor manipulation and its effects on metabolic flux redistribution in *Escherichia coli*. Metab Eng. 4, 182-192.

Sauer, U., Canonaco, F., Heri, S., Perrenoud, A., Fischer, E., 2004. The soluble and membrane-bound transhydrogenases UdhA and PntAB have divergent functions in NADPH metabolism of *Escherichia coli*. J Biol Chem. 279, 6613-6619.

Senior, P. J., Dawes, E. A., 1971. Poly-β-hydroxybutyrate biosynthesis and the regulation of glucose metabolism in *Azotobacter beijerinckii.* Biochem J. 125, 55-66.

Senior, P. J., Dawes, E. A., 1973. The regulation of poly-β-hydroxybutyrate metabolism in *Azotobacter beijerinckii*. Biochem J. 134, 225-238.

Soo, K. B., Chul, L. S., Yup, L. S., Nam, C. H., Keun, C. Y., Ihl, W. S., 1994. Production of poly(3-hydroxybutyric acid) by fed-batch culture of *Alcaligenes eutrophus* with glucose concentration control. Biotechnol Bioeng. 43, 892-898.

Stäubli, A., Boelsterli, U. A., 1998. The labile iron pool in hepatocytes: prooxidant-induced increase in free iron precedes oxidative cell injury. Am J Physiol Gastrointest Liver Physiol. 274, G1031-G1037.

Steinbüchel, A., 1991. Polyhydroxyalkanoic acids. In: Byrom, D., (Ed.), Biomaterials: Novel Materials from Biological Sources. Palgrave Macmillan UK, London, pp. 123-213.

Steinbüchel, A., Valentin, H. E., 1995. Diversity of bacterial polyhydroxyalkanoic acids. FEMS Microbiol Lett. 128, 219-228.

Stern, J. R., 1956. Optical properties of acetoacetyl-S-Coenzyme A and its metal Chelates. J Biol Chem. 221, 33-44.

Suhadolnik, R. J., Lennon, M. B., Uematsu, T., Monahan, J. E., Baur, R., 1977. Role of adenine ring and adenine ribose of nicotinamide adenine dinucleotide in binding and catalysis with alcohol, lactate, and glyceraldehyde-3-phosphate dehydrogenases. J Biol Chem. 252, 4125-4133.

Tan, D., Wu, Q., Chen, J.-C., Chen, G.-Q., 2014. Engineering *Halomonas* TD01 for the low-cost production of polyhydroxyalkanoates. Metab Eng. 26, 34-47.

Tolosa, L., Kostov, Y., Harms, P., Rao, G., 2002. Noninvasive measurement of dissolved oxygen in shake flasks. Biotechnol and Bioeng. 80, 594-597.

Vemuri, G. N., Altman, E., Sangurdekar, D. P., Khodursky, A. B., Eiteman, M. A., 2006. Overflow metabolism in *Escherichia coli* during steady-state growth: Transcriptional regulation and effect of the redox ratio. Appl Environ Microbiol. 72, 3653-3661.

Vollbrecht, D., Schlegel, H. G., Stoschek, G., Janczikowski, A., 1979. Excretion of metabolites by hydrogen bacteria. Eur J Appl Microbiol Biotechnol, 7(3), 267-276.

Vollbrecht, D., El Nawawy, M. A., Schlegel, H. G., 1978. Excretion of metabolites by hydrogen bacteria I. Autotrophic and heterotrophic fermentations. Eur J Appl Microbiol Biotechnol, 6(2), 145-155.

Vollbrecht, D., Schlegel, H. G., 1978. Excretion of metabolites by hydrogen bacteria II. Influences of aeration, pH, temperature, and age of cells. Eur J Appl Microbiol Biotechnol, 6(2), 157-166.

Wargo, M. J., 2013. Homeostasis and catabolism of choline and glycine betaine: Lessons from *Pseudomonas aeruginosa*. Appl Environ Microbiol. 79, 2112-2120.

Wargo, M. J., Szwergold, B. S., Hogan, D. A., 2008. Identification of two gene clusters and a transcriptional regulator required for *Pseudomonas aeruginosa* glycine betaine catabolism. J Bacteriol. 190, 2690-2699.

Wei, N., Quarterman, J., Kim, S. R., Cate, J. H., Jin, Y. S., 2013. Enhanced biofuel production through coupled acetic acid and xylose consumption by engineered yeast. Nat Commun. 4, 2580.

Wimpenny, J. W. T., Firth, A., 1972. Levels of nicotinamide adenine dinucleotide and reduced nicotinamide adenine dinucleotide in facultative bacteria and the effect of oxygen. J Bacteriol. 111, 24-32.

Ye, J., Hu, D., Che, X., Jiang, X., Li, T., Chen, J., Zhang, H. M., Chen, G.-Q., 2018. Engineering of *Halomonas bluephagenesis* for low cost production of poly(3-hydroxybutyrate-co-4-hydroxybutyrate) from glucose. Metab Eng. 47, 143-152a.

Ye, J. W., Huang, W. Z., Wang D. S., Chen, F. Y., Yin, J., Li, T., Zhang, H. Q., Chen, G. Q. 2018. Pilot scale-up of poly(3-hydroxybutyrate-co-4-hydroxybutyrate) production by *Halomonas bluephagenesis* via cell growth adapted optimization process. Biotechnol J. 13: e1800074b.

Yim, H., Haselbeck, R., Niu, W., Pujol-Baxley, C., Burgard, A., Boldt, J., Khandurina, J., Trawick, J. D., Osterhout, R. E., Stephen, R., Estadilla, J., Teisan, S., Schreyer, H. B., Andrae, S., Yang, T. H., Lee, S. Y., Burk, M. J., Van Dien, S., 2011. Metabolic engineering of *Escherichia coli* for direct production of 1,4-butanediol. Nat Chem Biol. 7, 445.

Yin, J., Wang, H., Fu, X.-Z., Gao, X., Wu, Q., Chen, G. Q., 2015. Effects of chromosomal gene copy number and locations on polyhydroxyalkanoate synthesis by *Escherichia coli* and *Halomonas sp*. Appl Microbiol Biotechnol. 99, 5523-5534.

Zhang J, Frerman F E, Kim J J P., 2006. Structure of electron transfer flavoprotein-ubiquinone oxidoreductase and electron transfer to the mitochondrial ubiquinone pool[J]. Proc Natl Acad Sci USA.103: 16212-16217.

Zhang, Y. H. P., 2008. Reviving the carbohydrate economy via multi-product lignocellulose biorefineries. J Ind Microbiol Biotechnol. 35, 367-375.

Tables and Figures

Table 1 Deletion and complementation of gene *etf* operon in *H. bluephagenesis* TD01

		Growth on GB		Growth on DMG	
Genotype	Predicted function	EV	CP	EV	CP
WT		+	N/A	+	N/A
Δβ	Electron transfer flavoproteins subunit β	-	+	-	+
Δα	Electron transfer flavoproteins subunit α	-	+	-	+

WT, wild type; GB, glycine betaine; DMG, dimethylglycine; EV, empty vector plasmid; CP, complementary plasmid; N/A, not applicable; −, poor growth; +, robust growth.

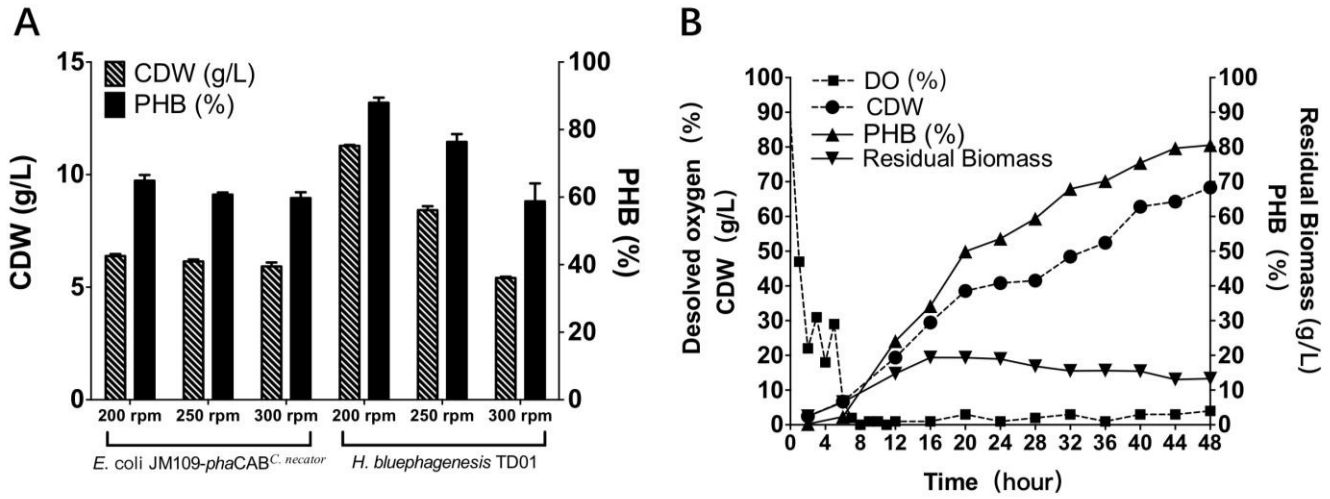

Figure 1 Oxygen limitation promotes PHB accumulation by *H. bluephagenesis* TD01

(A) Effect of shaking speed on growth and PHA synthesis by *E. coli* JM109 harboring *phaCAB* operon from *Cupriavidus nector* and *H. bluephagenesis* TD01 incubated on a rotary shaker, respectively. Data were obtained from three parallel studies (B) Effect of oxygen limitation on PHA synthesis by *H. bluephagenesis* TD01 grown in a 7 L fermentor under fed batch conditions. The agitation speed reached maximum of 800 rpm at 6 h, dissolved oxygen (DO) was maintained at 20% for 6 h by increasing 100 rpm each time, and was kept unchanged at 800 rpm after 6 h. The aeration was kept at 1 *vvm* during the entire process even though the actual DO remained approximately zero.

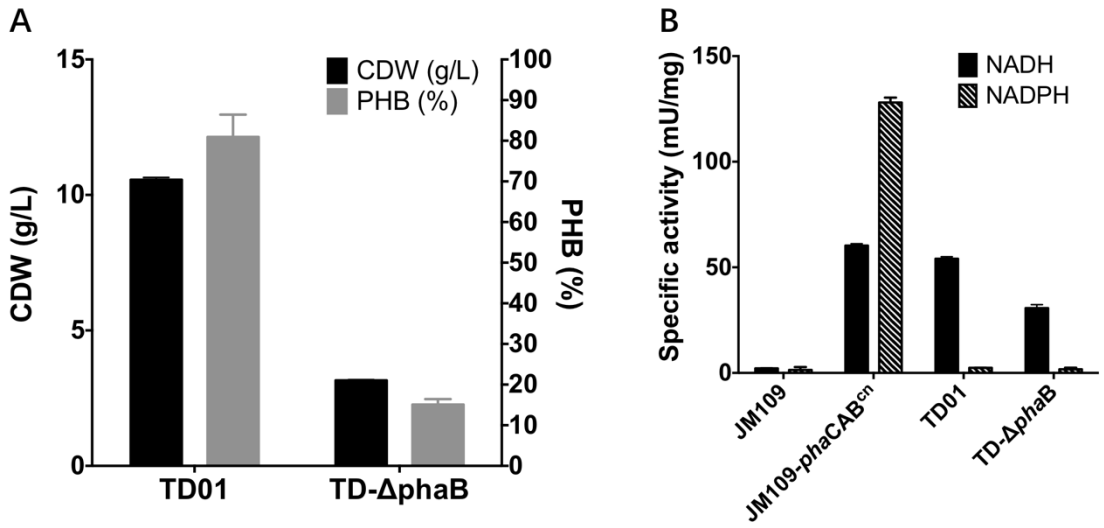

Figure 2 PhaB of *H. bluephagenesis* TD01 has almost no NADPH activity

(A) Grown and PHB synthesis by *H. bluephagenesis* TD01 and TD-Δ*pha*B incubated in shake flasks, respectively. The predicted main *pha*B of *H. bluephagenesis* TD01 was knocked out, the resulted mutant had much lower growth and PHB synthesis compared with that of the wild type. (B) Assays of specific enzymatic activities of PhaBs (acetoacetyl-CoA reductase, short as AAR) using acetoacetyl-CoA as the sole substrate, NADH and NADPH as the cofactor respectively. The PhaBs were from *E. coli* JM109 wild type, *E. coli* JM109 harboring *pha*CAB$^{C.\ necator}$, *H. bluephagenesis* TD01 and TD-Δ*pha*B, respectively. Statistics are obtained from average of at least 5 parallel studies, and error bars represent s.d.

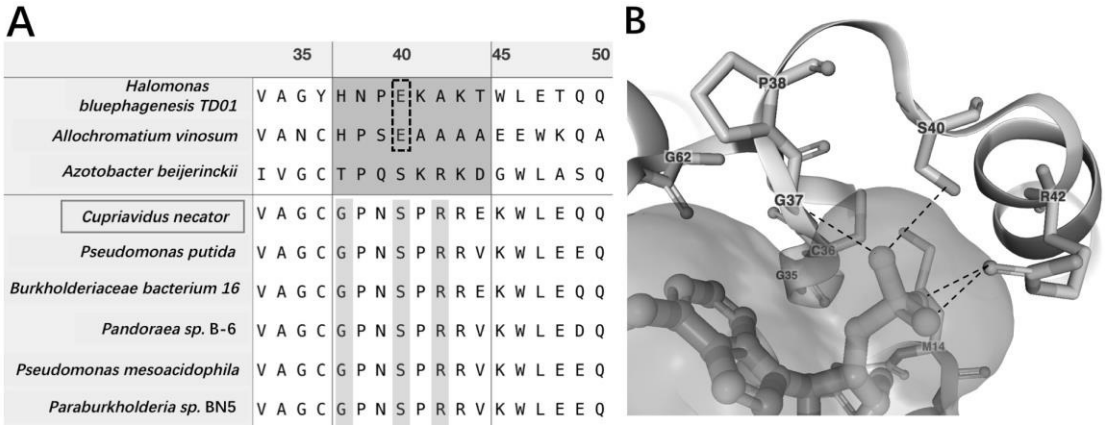

Figure 3 Analysis on amino acid sequences and structure of NAD(P)(H) binding domain of PhaBs from various organisms.

(A) Amino acid sequence alignments of NAD(P)(H) binding domain of PhaBs from *H. bluephagenesis* TD01, *Allochromatium vinosum* and *Azotobacter beijerinckii* compared to the PhaBs conserved in this domain of *Cupriavidus necator* and others. Amino acids marked in shadows are proven to form hydrogen bond to hydroxyl groups in the phosphate of NADP(H); these marked with black frames are suggested to form hydrogen bond to hydroxyl groups on the adenine ribose of NAD(H). The number of amino acids above was not the real order in any protein, they were generated during alignment in MATLAB. Same with the number in the structure in Figure 2B. (B) Structure of cnPhaB (PDB: 3VZP) in NADP(H) binding domain, G(37), S(40) and R(42) have been known to form hydrogen bonds with hydroxyl groups in the phosphate. The structure of cnPhaB was generated using NGL tool (https://github.com/arose/nglview) in RCSB Protein Data Bank (http://www.rcsb.org). The protein sequence is obtained from UNIPROT database.

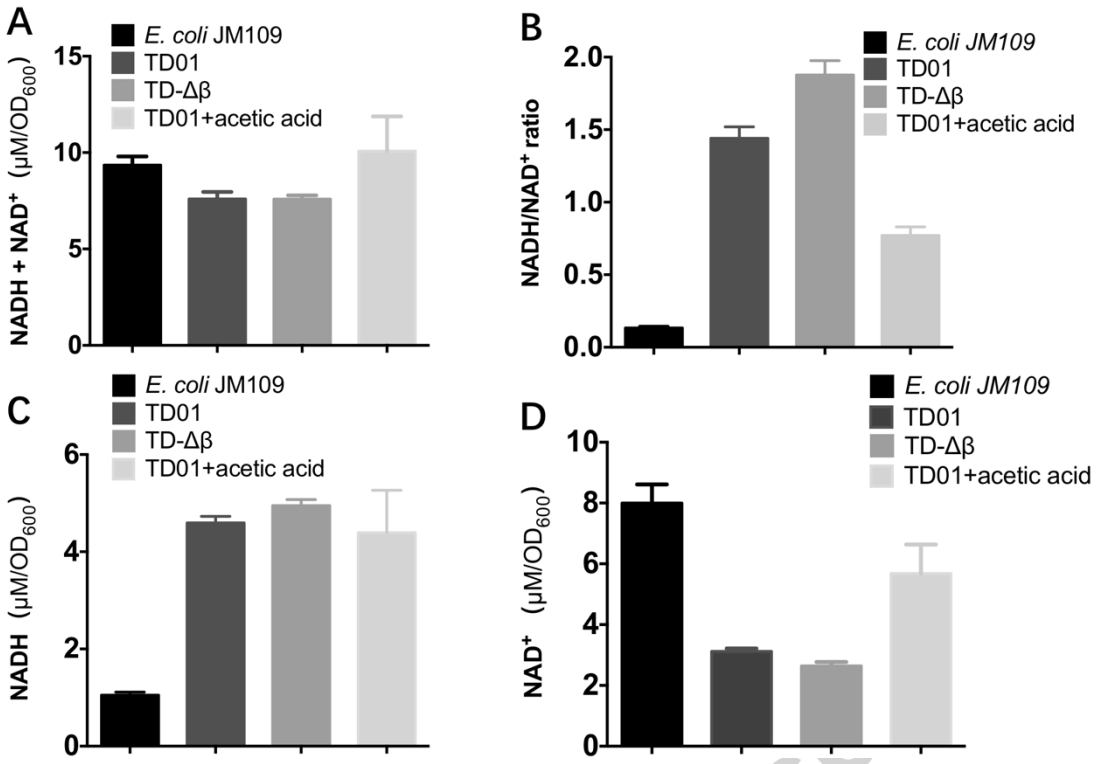

Figure 4 Studies on NADH and NAD^+ in *E. coli* JM109, *H. bluephagenesis* TD01, TD-Δβ grown in a LB medium, respectively.

(A) Total NADH and NAD^+ pools of *E. coli* JM109, *H. bluephagenesis* TD01 and TD-Δβ as well as TD01 grown in the LB medium added with 2 g/L acetic acid, respectively. (B) NADH/NAD^+ ratios in *E. coli* JM109, *H. bluephagenesis* TD01 and TD-Δβ as well as TD01 grown in the LB medium added with 2 g/L acetic acid, respectively. (C) NADH amounts in *E. coli* JM109, *H. bluephagenesis* TD01 and TD-Δβ as well as TD01 grown in the LB medium added with 2 g/L acetic acid, respectively. (D) NAD^+ amounts in the four groups. Statistics are obtained from at least 5 parallel studies, and error bars represent s.d.

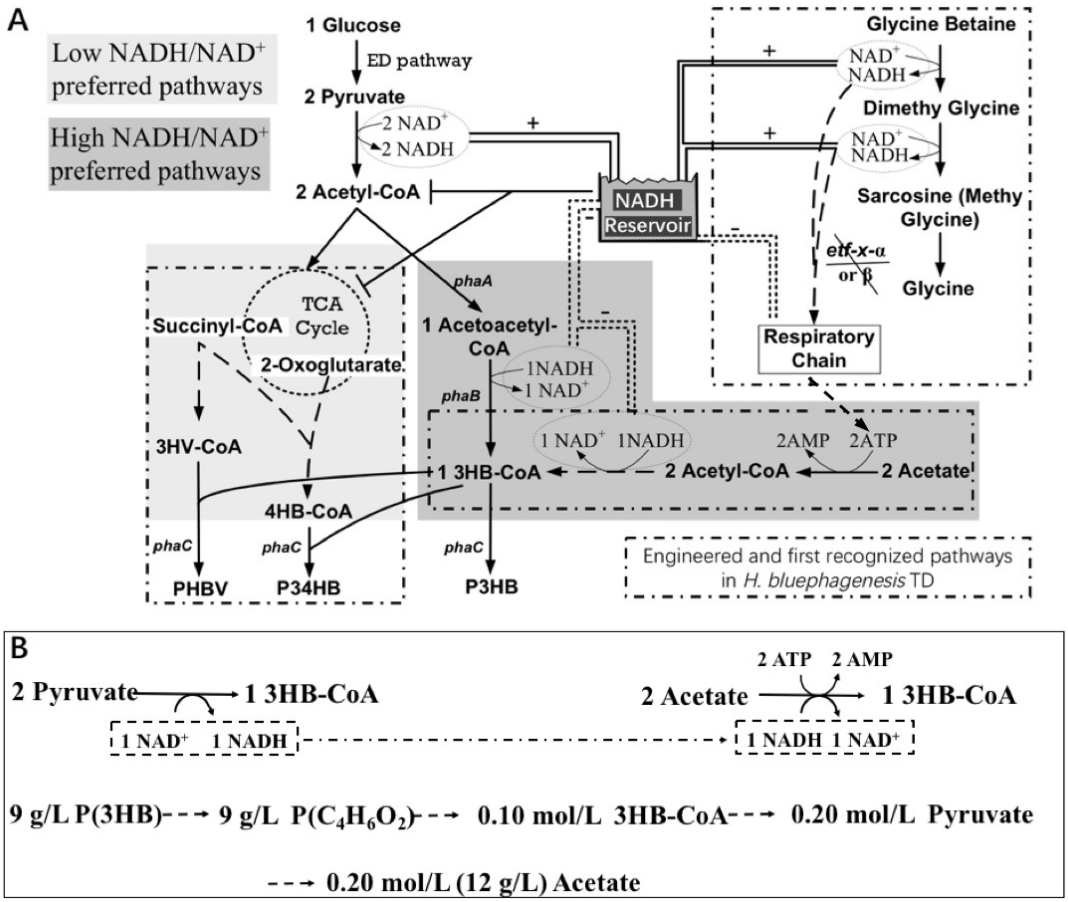

Figure 5 Engineering NADH reservoir for enhanced synthesis of PHB, P34HB and PHBV by *etf* mutated *H. bluephagenesis*, respectively

(A) Metabolic pathways of PHB, P34HB and PHBV synthesis in engineered *H. bluephagenesis*. PHB was synthetized directly from acetyl-CoA via NADH dependent fermentative pathway. Whereas copolymer P34HB and PHBV syntheses could be divided into two parts containing 3HB synthesis pathway favoring high NADH/NAD$^+$ ratio and a TCA cycle related pathway, namely 4HB and 3HV synthesis pathway requiring intermediates from TCA cycle, which would be inhibited by NADH under oxygen limitation. Mutation on *etf-x* enhances NADH/NAD$^+$ ratio, channeling more acetyl-CoA to PHB synthesis. Acetate can function as a sink of NADH and redox regulator to balance the NADH reservoir to enhance acetyl-CoA concentration. (B) Calculation of NADH in PHB synthesis pathway: One NADH is generated when one 3HB-CoA is formed from 2 pyruvates, one NADH is consumed when two acetic acid molecules are reduced to 3HB-CoA. 30 g/L glucose as the carbon source led to approximately 9 g/L PHB during shake flask studies, requiring 0.2 mol/L pyruvate, 12 g/L acetic acid could be reduced by the redundant NAD

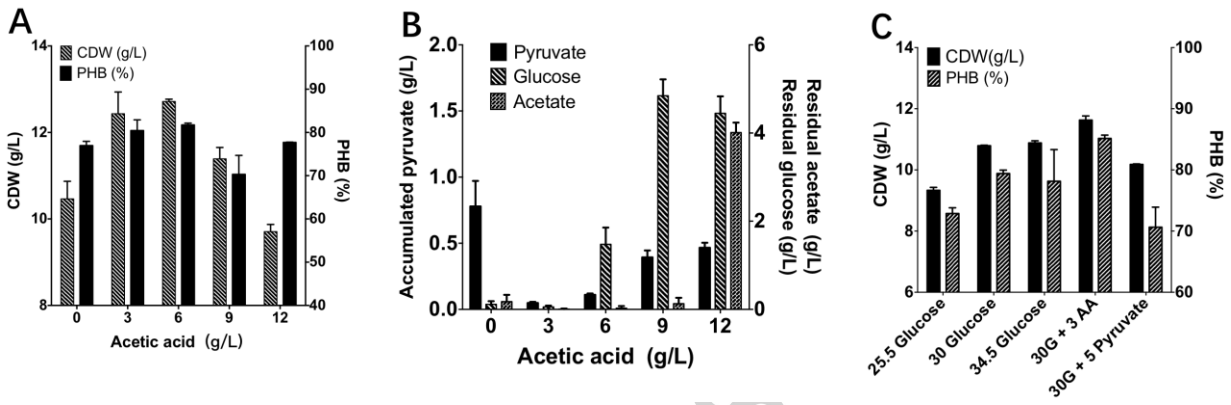

Figure 6 Effect of acetic acid on growth and PHB synthesis by *H. bluephagenesis* TD01 incubated in a glucose medium

(A)(B) Growth and PHB synthesis by *H. bluephagenesis* TD01 incubated on a rotary shaker (200 rpm) in a 30 g/L glucose (G) medium in the presence of 0-12 g/L acetic acid (AA), respectively. (C) Growth and PHB synthesis by *H. bluephagenesis* TD01 incubated on a rotary shaker (200 rpm) in the presence of various substrates, respectively. Statistics are obtained from at least 5 parallel studies, and error bars represent s.d.

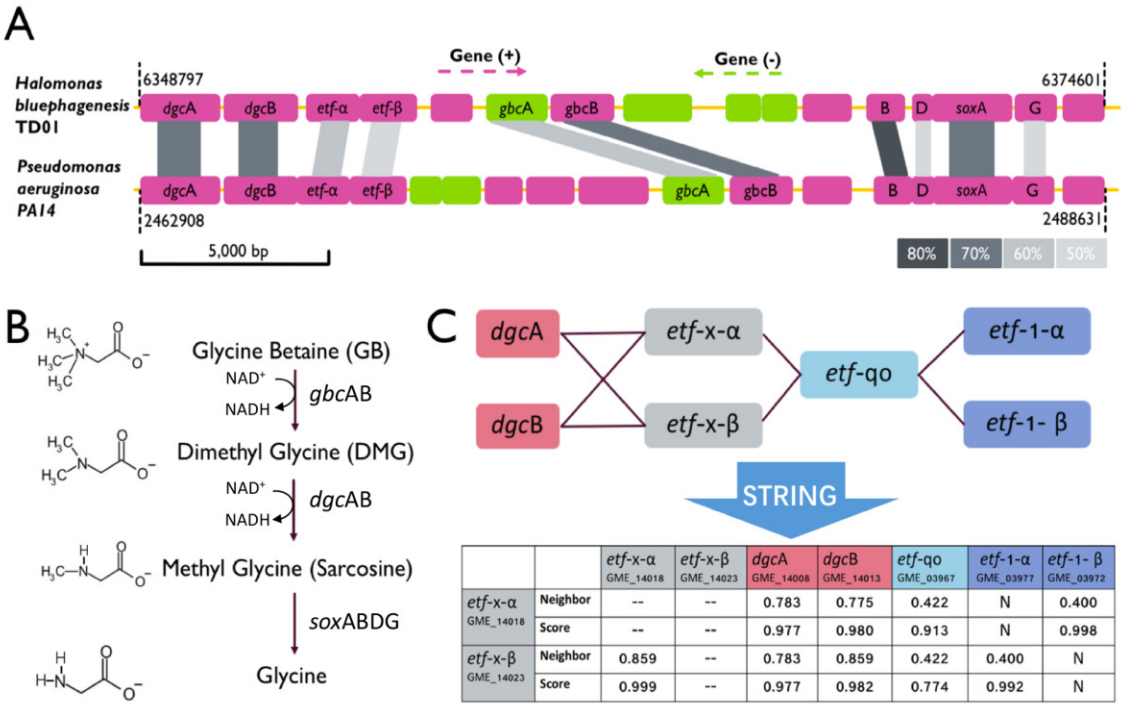

		etf-x-α GME_14018	etf-x-β GME_14023	dgcA GME_14008	dgcB GME_14013	etf-qo GME_03967	etf-1-α GME_03977	etf-1- β GME_03972
etf-x-α GME_14018	Neighbor	--	--	0.783	0.775	0.422	N	0.400
	Score	--	--	0.977	0.980	0.913	N	0.998
etf-x-β GME_14023	Neighbor	0.859	--	0.783	0.859	0.422	0.400	N
	Score	0.999	--	0.977	0.982	0.774	0.992	N

Figure 7 Bioinformatic analysis of the relationship between *etf*-x genes encoding electron transfer flavoproteins and genes related to glycine betaine (GB), dimethylglycine (DMG) metabolisms. (A) Comparative genomic analysis of genes neighbor to *etf*-x between *H. bluephagenesis* TD01 and *Pseudomonas aeruginosa* PA14, revealing that genes around *etf-x* participate in metabolisms of glycine betaine (GB) and dimethylglycine (DMG). (B) Proposed metabolic pathway from glycine betaine to glycine in *H. bluephagenesis* TD01. (C) Systematic assessment of functional and physical correlations between *etf-x* and genes in GB+DMG metabolism as well as the conserved *etf*-qo, respectively, in genome of *H. bluephagenesis* TD01 using STRING database. Neighborhood and total scores denote physical correlation and comprehensive correlation between two genes in one bacterium, respectively. The gene operon *sox* is the abbreviation of sarcosine oxidase.

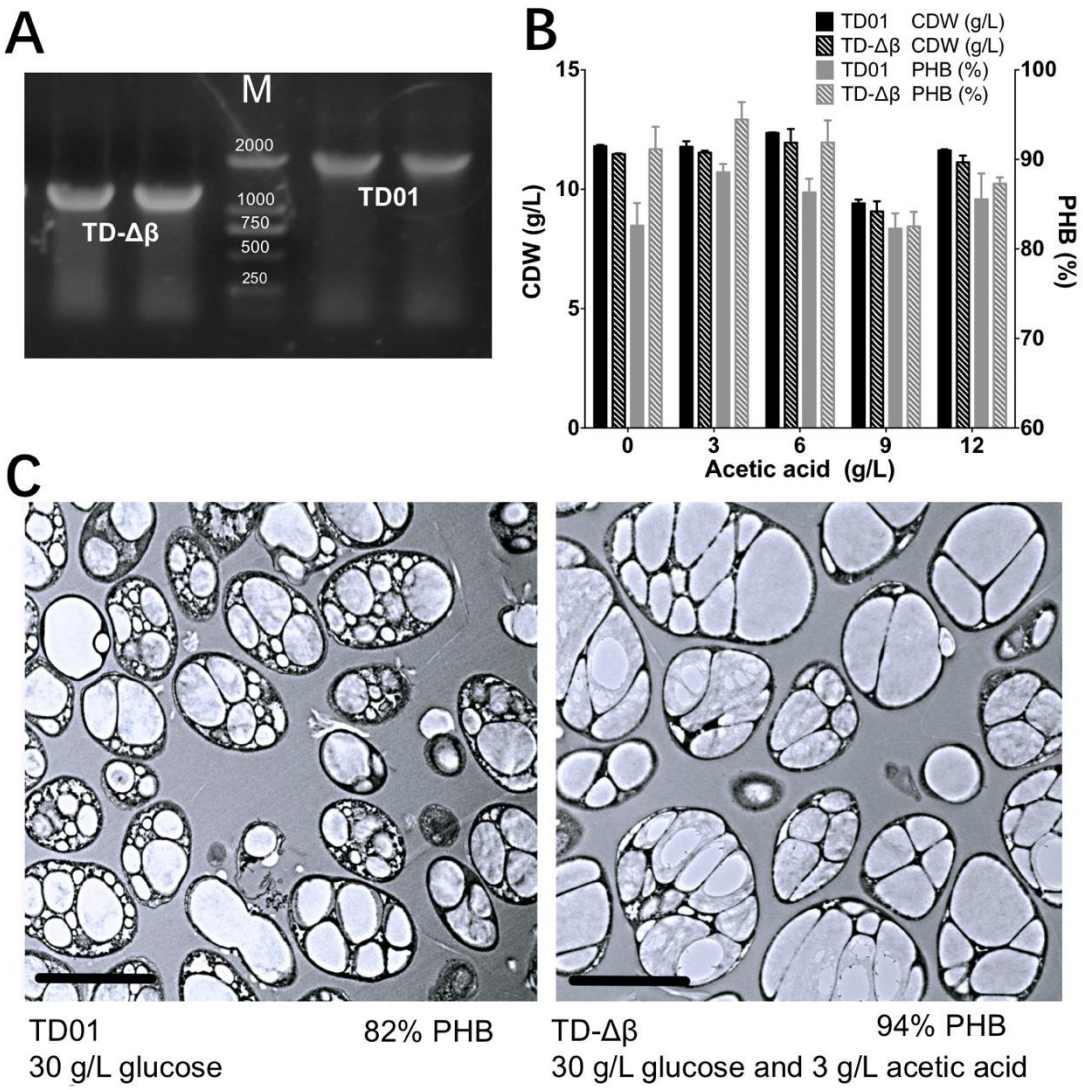

Figure 8 Deletion on *etf*-x in *H. bluephagenesis* enhance its PHB accumulation

(A) The gene *etf-x*-β was deleted via CRISPR/Cas9, M represents marker, the bands of wild type on the right and *H. bluephagenesis* TD-Δβ on the left are 1962 bp and 1231bp, respectively. (B) *H. bluephagenesis* TD01 and TD-Δβ grown in 30 g/L glucose in the presence of gradient concentrations of acetic acid. (C) TEM images of *H. bluephagenesis* TD01 and TD-Δβ accumulated with PHB granules, respectively. The scale bar is 2 μm.

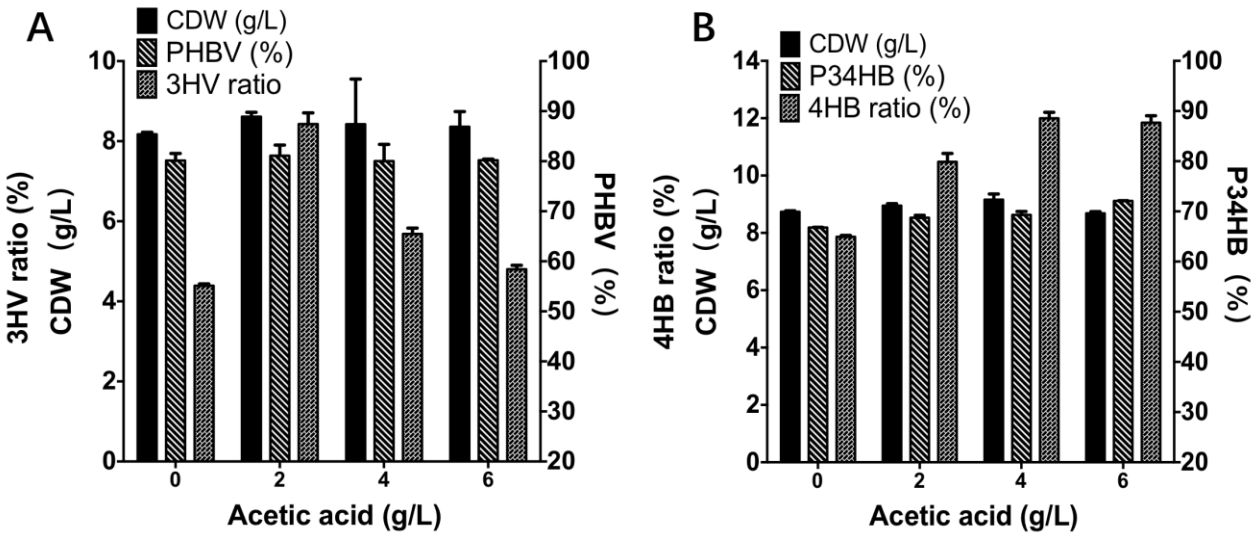

Figure 9 Effect of acetic acid on growth, PHBV and P34HB syntheses by recombinant *H. bluephagenesis* strains incubated in 30 g/L glucose medium, respectively.

Statistics are obtained from at least 5 parallel studies, and error bars represent s.d.

Highlights：

1. PhaB is found to be a NADH dependent enzyme for PHB synthesis in *Halomonas bluephagenesis*
2. Oxygen limitation was proven to promote PHA accumulation
3. Acetic acid helps enhance PHA production and control the monomers ratios in copolymers
4. Deletion of an unessential set of *etf* further increases PHA accumulation